Routledge
Taylor & Francis Group

Journal of Environmental Planning and Management

ISSN: (Print) (Online) Journal homepage: www.tandfonline.com/journals/cjep20

IoT sensors as a tool for assessing spatiotemporal risk to extreme heat

Kijin Seong, Seung Jun Choi & Junfeng Jiao

To cite this article: Kijin Seong, Seung Jun Choi & Junfeng Jiao (15 Mar 2024): IoT sensors as a tool for assessing spatiotemporal risk to extreme heat, Journal of Environmental Planning and Management, DOI: 10.1080/09640568.2024.2320257

To link to this article: https://doi.org/10.1080/09640568.2024.2320257

Journal of Environmental Planning and Management, 2024
https://doi.org/10.1080/09640568.2024.2320257

Routledge
Taylor & Francis Group

IoT sensors as a tool for assessing spatiotemporal risk to extreme heat

Kijin Seong, Seung Jun Choi* and Junfeng Jiao

Urban Information Lab, The School of Architecture, The University of TX at Austin, Austin, TX, USA

(*Received 9 December 2022; final version received 12 February 2024*)

The safety of urban populations sensitive to extreme heat is under increasing threat. Few studies examine the potential benefits of deploying IoT environmental sensors in the urban context and their integration with large-scale human activity data. This paper examines the deployment of IoT sensors in high-resolution extreme heat risk assessment in the case of Seoul, South Korea. This study conducted spatiotemporal analysis on heat exposure with IoT sensors, compared it with an existing land surface temperature map for validation, combined it with human activity data for risk assessment, and finally discussed the benefits of IoTs in detecting abnormal weather events. The results show that extreme heat risks and characteristics vary by age group, and socio-demographic nature overlaps with contextual factors concerning climate risk. This paper discussed possible policy implications to better deal with recurring climate hazards using IoT sensors.

Keywords: extreme heat; heat exposure; IoT; de-facto population; climate resilience

1. Introduction

The growing frequency and intensity of extreme heat caused by climate change is a serious public concern threatening the living environment in Seoul, South Korea. Extreme weather events require long-term efforts to overcome challenging issues associated with the recovery process (Sima, Thomas, and Lowrie 2017). Repeated extreme summer heatwaves can have a fatal impact on an individual's daily life which is now considered the "New Normal" that calls for consistent attention (Sima, Thomas, and Lowrie 2017; Perkins-Kirkpatrick and Gibson 2017). In line with concerns associated with recurring climate calamities, there is growing awareness about the public health concerns of vulnerable populations – including the elderly, children, the disabled population, households below the poverty line, and racial minorities – who may be susceptible to extreme weather events (Aubrecht *et al.* 2013; Depietri, Welle, and Renaud 2013; Wilson and Chakraborty 2019; Nayak *et al.* 2018). Extreme heat disproportionally burdens the historically disadvantaged population such as communities of color and low-income neighborhoods (Chakraborty *et al.* 2022). Thus, it is critical to address the occurrence pattern of extreme weather events and identify spatiotemporal exposures to the risks among vulnerable populations to mitigate the potential climate risks.

Utilizing new technologies in the context of smart cities improves, expediting governance, economic, social, and environmental decision-making, and service delivery,

*Corresponding author. Email: jun.choi@utexas.edu

all for the public benefit (Nica 2021). Accordingly, the Seoul Metropolitan Government has installed S-DoTs (Smart Seoul Data of Things) throughout the city since 2020 to collect microscopic real-time climate data to detect, diagnose, and prevent extreme weather events.

This paper aims to explore the deployment of Internet of Things (IoT) environmental sensors as a tool to estimate heat risks in the case of Seoul, South Korea. First, this study addresses how high-resolution IoT sensors can improve the identification of heat exposure patterns through spatiotemporal analysis, compared to the existing tool using satellite images. Second, the study examines extreme heat risk assessment by age groups with human dynamics data. And finally, this study will discuss the benefit of IoTs in identifying abnormal weather events using machine learning and how it can be used for environmental planning and management.

2. Extreme heat and IoT environmental sensors

Extreme heat refers to periods of extreme warmth that directly affect human health (Smith, Zaitchik, and Gohlke 2013). Prolonged exposure to high temperatures is a risk factor for heat-related disorders, including heat cramps, heat syncope, heat exhaustion, heatstroke, and mortality (Kim *et al.* 2014, 2016; Lee *et al.* 2016). Despite its severity, heat-related illnesses and mortality occur unequally. Socioeconomically vulnerable groups are generally more at risk because of their lack of *capability* to deal with high-temperature exposure (Kim and An 2017; Wilson and Chakraborty 2019). Age is a significant factor that increases heat exposure sensitivity. For instance, the elderly's chronic diseases or incapability to control increasing temperature (Basu and Ostro 2008), infants, children, and adolescents' sensitive metabolic activities, create higher heat and lower cardiac output than adults (Bytomski and Squire 2003; Krous *et al.* 2001). In addition, working populations in poverty or living alone in Korea face a higher vulnerability to extreme heat events. Those in poverty often work as day laborers in outdoor environments, where they face inadequate protection against heat and may lack air conditioning. As of 2022, the number of households in Seoul receiving basic living subsidies is 308,484, accounting for 8% of the total households (Seoul Metropolitan Government 2022). In Seoul, 44.9% of the households in poverty, with an income less than 50% of the median income, are non-economically active, and even those who are economically active are mostly day laborers (Kim and Dong Yeol 2015). There are no guidelines established for heatwave preparedness in day laborers in outdoor environments (Korea Institute for Health and Social Affairs 2020). Heatwave-related deaths of working groups aged 20–64 years are mainly outdoor workers (Kim *et al.* 2017). Korea Institute for Health and Social Affairs (2020) conducted surveys and interviews to develop measures to minimize health damage during heatwaves. Among the surveyed 375 respondents in poverty, they lacked air conditioning the most by 14.1% while only 2.5% of the other 1,125 respondents not in poverty lacked air conditioning. Even with air conditioning available, 68.6% of the respondents in poverty reported that they refrained from using it due to financial burdens. Similarly, individuals living alone might not have immediate access to assistance or medical aid in the event of heat-induced illnesses (Kim and An 2017; Kwon, Lee, and Kwon 2020).

Heat risk analysis requires spatial and temporal observations (Voogt 2007). The most popular technique for collecting temperature data for heat exposure analysis includes estimating temperature using remote sensing images, measuring by mobile

transect observation, and utilizing fixed weather station equipment data (Sun *et al.* 2014). Each of these has limitations in spatial and temporal observations. First, collecting temperature data from satellite images has poor data continuity due to the satellite's orbital period and cloud cover (Sobrino and Raissouni 2000). Especially in the summertime when heat risk study is critical; it is even worse due to the higher cloud coverage ratio in the rainy season, restricting temporal data accessibility (US Geological Survey 2018). Another constraint is that the temperature might somewhat differ from the real temperature since it is an anticipated value based on surface radiation energy rather than a measured one (Kim and An 2017). The second method of obtaining temperature data directly with mobile transect observation is also difficult to gather data over a large territory, given that it requires a well-planned measurement route, appropriate type of transportation, careful control of measurement timing or data time correction, and the regular speed of the mobile platform (Sun *et al.* 2014). Finally, weather observation equipment, such as Automatic Weather System (AWS), are widely apart for spatial interpolation; thus the projected values may range greatly from the real temperature (Kim and An 2017; Ku 2014).

Based on the existing limitations, deploying urban sensors for temperature collection has been newly attempted. IoT is defined as universally connected devices that exchange information and communicate using internet-based protocols (Patel, Patel, and Scholar 2016). Researchers argue that heat risk analysis using high-density IoT sensors is useful for implementing and evaluating efforts to alleviate the technical issues with current means of measurement, eventually leading to mitigating urban climate problems with heterogeneous and diverse characteristics (Muller *et al.* 2013; Smoliak *et al.* 2015). Exclusively relying on a single source to measure potential environmental harm could result in biases (Chakraborty *et al.* 2022). Given that, utilizing IoT devices is a vital component of smart city planning efforts for climate resilience (Sehrawat and Gill 2019; Rathore, Ahmad, and Paul 2016).

Generally, IoT sensors enable a more precise delineation of the urban heat landscape and aid in identifying the temporal and spatial patterns of populations at heightened risk from extreme heat events. The delineation can range from minute-level to hourly data, which allows for a detailed analysis of heat exposure risks at different times of the day. The importance of utilizing higher resolution data lies in its ability to capture the fluctuations in temperature throughout the day in Seoul. The annual mean air temperature in Seoul is 12.5 °C, reaching its highest in summer (June-August) at 24.3 °C (Zheng, Yu *et al.* 2020). This period is also when Tropical Nights (TN) with temperatures greater than 25 °C become severe in Seoul. On TN days, the hourly air temperature ranges from 26 °C at 6 am to over 30 °C at 12 pm and on non-TN days, the hourly temperature varies from around 20 °C at 5–6 am, peaking at 30 °C at 3 pm in July and August (Ha and Yun 2012). Addressing temperature variability is crucial for assessing health risks, as the impact of heat on health can be immediate or delayed, with potential lag effects (Watson, Gardiner, and Singleton *et al.* 2020). Response of heat-related emergency medical services are temporally and spatially affected with most delayed responses in the morning and the evening hours (Seong, Jiao, and Mandalapu 2023).

Although previous studies have attempted to use spatiotemporal information derived from IoTs to examine the distribution of heatwaves (Fauzandi *et al.* 2021; Husni *et al.* 2022; Yu, Shen, and Cervone 2022), limited research has addressed the benefits of IoT sensors surpassing existing means of temperature measurement and its validation, the

integration with other data sources (i.e. meteorological data from weather stations, satellite imagery, geospatial data, and even social media data for crowd-sourced weather observations), and the detection of extreme weather events due to the short installation and operation period of IoT sensors in many cities. Hence, this study will provide evidence of the potential benefits of IoT sensors in extreme heat detection and management and suggest how it can be utilized for environmental research.

3. Materials & methods

3.1. Study area & S-DoT distribution

This study chose Seoul as a study area for two reasons. First, Seoul has the highest density of IoT environmental sensors than any other city in the world. As of 15 June 2021, 1,060 Smart Seoul Data of Things (S-DoTs) are operating in Seoul, and Seoul Metropolitan Government aims to install up to 2,500 S-DoTs by 2022 as a part of Seoul's smart city vision plan (Figure 1). S-DoTs can measure weather variables, such as particulate matter, temperature, illuminance, noise, vibration, wind speed, and wind direction in the atmosphere. The data collected by S-DoTs is openly accessible through the Open Data Portal operated by the Seoul Metropolitan Government. The time unit of the provided data is hourly. It is evenly distributed throughout Seoul's administrative boundaries, which provides a perfect case for urban IoT sensor studies. Second, the mismatch between the registered population and actual human activity in Seoul offers a good example of how human dynamics data could be used for de facto risk exposure. Specifically, Seoul used to have a registered population of 10 million; however, it fell below for the first time in 2021. Despite its smaller size than other global megacities, Seoul's population density is 16,751 people per square kilometer,

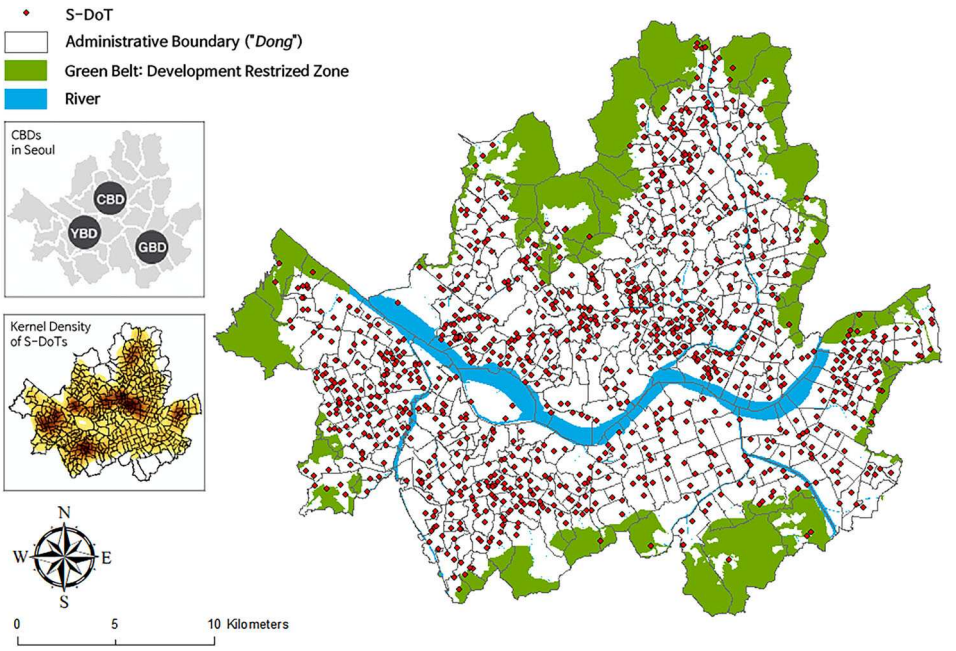

Figure 1. Study area.

approximately 2.4 times more than NYC, ranging from 310 to 54,847 people per square kilometer among 424 administrative boundaries (Lee, Jiao, and Choi 2021). Considering the population movement who spend their daily routines in Seoul for work, school, or visit for leisure purposes, the number surpasses the registered population. In brief, the high density of IoT environmental sensors and the increase in human activity than registered population makes Seoul a perfect case area for this study.

3.2. Data collection

3.2.1. S-DoT data analysis and curation

The study period is from 1 June 2020 to 31 August 2020. This study collected S-DoT data during the date with extreme heat advisory alerts in effect. We focused on atmospheric temperature data read by deployed S-DoTs. According to Korea Meteorological Administration, seventeen extreme heat advisory alerts were announced in Seoul during the study period. Advisory alerts in effect during the study period are summarized in Appendix 1.

The integration of S-DoT data into meteorological condition evaluations offers several benefits. Park and Baek (2023) note that the horizontal operational network of S-DoTs (0.75 km) surpasses that of Automated Weather Systems (AWS) and the Automated Synoptic Observing System (ASOS). The S-DoTs are evenly installed across administrative boundaries within Seoul (Park and Kim 2020; Park and Baek 2023). The highly resolute temperature enables a more accurate meteorological assessment (Kim and Kang 2022; Park and Baek 2023).

The data pre-processing went through the following steps. First, we imported the coordinates of individual S-DoTs into ArcMap, and using the spatial join operation, we then associated each S-DoT with its respective spatial location information, using the WGS84 coordinate system (EPSG: 4326). Second, the 17 days of records obtained were imported in Python. Numpy (Harris *et al.* 2020) and Pandas (Reback *et al.* 2022) modules were used. The joined spatial information was merged into the original records based on the unique serial code of S-DoT. Third, the joined data frame was grouped by an added geographic unit: administrative boundary and DateTime to gather the hourly average atmospheric temperature for all 424 administrative boundaries in Seoul. Ideally, there should be 10,176 records (424 administrative boundaries $\times$ 24 h). However, 608 records were missing, accounting for approximately 5.9% of the total observations. Although this magnitude is small, we performed mean substitution on these missing observations to utilize the complete dataset. Rather than using the incomplete data frame, our study generated a new one, a combination of 424 administrative boundaries and 24 h. We merged the incomplete data frame with the complete one and conducted mean substitution based on the hourly average atmospheric temperature.

3.2.2. Human dynamics data

Due to the advancement of telecommunication technology, mobile phone devices are widely used in our daily routines. The real-time data collected by these devices can represent a de facto human activity, as most people carry phones all the time. Instead of using static census data, human activity data represent real-time de facto population movement and travel patterns (Song *et al.* 2010). Recently, the use of human activity data has increased in urban research, including studies examining travel behaviors and

patterns (Lee, Choi, and Jiao 2021; Song *et al.* 2010; Chen and Yeh 2022), optimization for small businesses (Cho and Lee 2022), demands for urban facilities (Baz-Lomba *et al.* 2019), and neighborhood vitality (Kang 2020; Barbour *et al.* 2019).

Seoul Metropolitan Government publicizes mobile phone signal-based human dynamics data. The spatiotemporal characteristics of human dynamics data have been well documented by Lee, Jiao, and Choi (2021), who utilized the data as a proxy to measure real-time spatiotemporal transportation service demand.

In human dynamics data, human activity is classified into gender (male/female) and different age groups. It is provided across all administrative boundaries in Seoul. We collected human dynamics data during the same period when heat advisory alerts were in effect during the study period and selected the time period of 3 pm, when the temperature typically reaches its peak. This study defined three age groups which are youth (age under 15), elders (age over 64), and working population (age older than 15 and younger than 64, inclusive). Then, human dynamics data were subset summed for the corresponding age group.

3.3. *Methods*

3.3.1. *Spatiotemporal analysis*

This study used urban climate sensor data and human dynamics data (Table 1) to address extreme heat spatiotemporal analysis in Seoul, South Korea. The research went into two phases. First, the hourly average atmospheric temperature of extreme heat during advisory alerts was analyzed in time series. Second, the total hourly average temperature, derived from the hourly averaged data during the advisory alerts, was subjected to descriptive spatial analysis. We conducted a hot spot analysis tool in ArcMap to perform a Getis-Ord Gi analysis, enabling us to identify the spatially significant clusters of hot and cold spots (ESRI 2023). We established peak hours based on a temporal analysis of the average hourly temperatures collected during advisory alerts. In this context, the term "peak hours" specifically refers to the timeframe from 12 pm to 6 pm, which was determined to be the period that consistently exhibited the highest temperatures.

3.3.2. *Kriging interpolation and correlation analysis*

We conducted universal kriging using ArcMap to expand the point observation to cover the entire study area. Previous studies on ambient temperature have predominantly utilized Universal Kriging (Caballero, Giraldo, and Mateu 2013; Hudson and Wackernagel 1994; Roznik *et al.* 2019). Hourly mean temperature during the study period was employed. 3 pm was chosen to represent the extreme heat risk in peak hours. To determine the land surface temperature (LST), this study utilized Landsat 8 satellite image on 23 June 2017, which was the most recent date available based on both land cloud coverage ($< 20\%$) and the date corresponding to the specific day designated as an extreme heat advisory alert.[1] The LST was calculated through methods in previous studies (Avdan and Jovanovska 2016). Finally, a fishnet (50×50) was created to collect observations across locations. And the LST values from the Landsat8 image and the S-DOT average air temperature data were normalized to a common baseline to account for the temporal and spatial differences between the datasets. We employed min-max normalization, which scales the data from 0 to 1. Points outside the study area were removed prior to correlation analysis between two datasets.

3.3.3. Risk assessment

This study calculated the Z-score of the average temperature and human dynamics during the peak hour periods throughout periods of extreme heat alerts. Peak hour periods were determined after temporal analysis using total hourly average temperature, derived from the hourly averaged data during the advisory alerts. Peak hours were identified through a temporal analysis, where the average hourly temperature was calculated using data collected during advisory alerts. This analysis defined the peak hours as the period from 12 pm to 6 pm, which encompasses the three hours before and after the hottest time of the day. We also gathered data on human dynamics throughout this same period. Additionally, the average was taken from two distinct sources within the administrative boundaries of Seoul. The Z-score was calculated by subtracting each scale from the average and dividing it by the standard deviation. It tells how far each observation is above or below average (Lee, Jiao, and Choi 2021). The (+) positive value means that the observation is greater than the mean, whereas the (−) negative value indicates that the observed data is lower than the average. Several previous studies employed the z-score approach to map heat-related risks (Christenson *et al.* 2017; Zheng, Zhang *et al.* 2020). After calculating two Z-scores – one from the average temperature and the other from human dynamics during peak hours – we computed the mean of these two Z-scores. The averaged Z-score used for the assessment was broken down into ten quantile breaks (10%) in ArcMap. This calculation involves addressing the relativity of risk during extreme heat events. The final average Z-score calculation goes through the flowing equation:

$$\mathrm{Z-Score\ of\ Risk\ Assessment}_{\rho} = \mathrm{AVG}\ (\mathrm{Z-Score}_{\rho} + \mathrm{Z-Score}_{\sigma})$$

(ρ: Temperature; σ: Human dynamics of heat advisory alert days for each ρ)

Fourth, this study conducted an independent T-test to address how Seoul's socioeconomic characteristics and planning implications relevant to the lowest and highest risk areas are statistically different. The variables collected for the independent T-test are openly accessible from the Open Data Portal provided by the Seoul Metropolitan Government, which include socio-demographic, urban greenness and heat infrastructure factors shown in Appendix 2. In addition, we carried out a T-test to compare the mean proportions of human dynamics across various age groups during peak hours. The independent T-test uses the following equation:

$$\mathrm{t} = \frac{\underline{X_H} - \underline{X_L}}{SE_{\underline{X_H} - \underline{X_L}}} \tag{1}$$

where $\underline{X_H}$: Average of the Highest Risk; $\underline{X_L}$: Average of the Lowest Risk; $SE_{\underline{X_H}} - \underline{X_L}$: Standard Error of the Highest Risk & the Lowest Risk.

We used Python, ArcMap 10.8, Stata 11, and Tableau Desktop for technical support. Appendix 2 summarizes a descriptive statistic for variables used in the independent T-Test analysis.

3.3.4. Isolation forest for anomaly detection

After identifying spatiotemporal exposure to extreme heat in Seoul, we conducted anomaly detection using an Isolation Forest (IForest). To address the worst-case scenario, we examined zones previously believed to house a significant number of low-income seniors. We aimed to determine whether there were any unusual instances of

excessive heat exposure in these vulnerable areas. IForest is an unsupervised machine-learning algorithm that identifies anomalies by constructing trees. In IForest, anomalies refer to the observation that depicts dissimilar characteristics to the normal instances, which occur in only a few instances (Liu, Ting, and Zhou 2008). The anomaly score is calculated as follows:

$$S(x,n) = 2^{\frac{-E(h(x))}{c(n)}} \tag{2}$$

where, S : anomarly score of instance x; $h(x)$ is a path length of instance x; $E(h(x))$ is a mean of $h(x)$ from all trees; the denominator $c(n)$: is a mean tree depth of an unsuccessful search calculation which is calculated as follows:

$$2H(n-1) - \left(\frac{2(n-1)}{n}\right) \tag{3}$$

where n is the total number of data points; $H(i)$ is a harmonic number calculated by an Euler's constant $(\ln(i) + 0.5772156649)$.

IForest necessitates the setting of constant hyperparameters, often referred to as contamination. This term can also be synonymous with biases. Our study adopted the approach by Hasan *et al.* (2019), which outlines the typical sensor malfunction frequency rate of 2.76%. We used this rate as the malfunction rate for S-DoTs was not clear. In addition, for other hyperparameters, 70% of the data were used for training, and the number of base estimators was set to 200. A random seed number of 1 was used to repeat the sequence. Our study evaluated the anomaly detection in two instances; (1) where the instance is greater than the mean temperature in peak hours in Seoul (higher than 33.33 °C), and (2) where the instance is greater than the standard of initiating extreme heat alert (higher than 35.00 °C). IForest was imported from the Scikit-learn module (Pedregosa *et al.* 2011) using Python.

4. Results

4.1. Spatiotemporal analysis of extreme heat through S-DOT

Figure 2 illustrates the average temperature during the heat advisory alerts by administrative boundaries. Despite its existing variation, administrative boundaries in Seoul shared a similar hourly pattern in average temperature. The average temperature would go up after 7 am, hit its peak in the afternoon (3 pm), and start declining. The lowest observed point was 6 am with an average of 26.10 °C, ranging from 22 °C to 27 °C, while the highest averaged observation was 33.33 °C at 3 pm, ranging from 31.0 °C to 35.0 °C. We defined the hour periods from 12 pm to 6 pm as peak hour periods for extreme heat.

Figure 3 shows the descriptive spatial analysis of the total hourly average temperature measured by S-DoTs. For clarification, the total hourly average employed for the spatial analysis encompasses all records collected during the hours when the advisory alerts were in effect. The temperature is relatively high in the central business district (CBD) and the Eastern part of Seoul. The hot spot analysis result reveals clear clustering and dispersion patterns with statistical significance. Clusters of hot spots relevant to temperature are figured in Seoul's Eastern, Central, North-western, and South-eastern sides. The occurrence patterns and characteristics of different temperatures

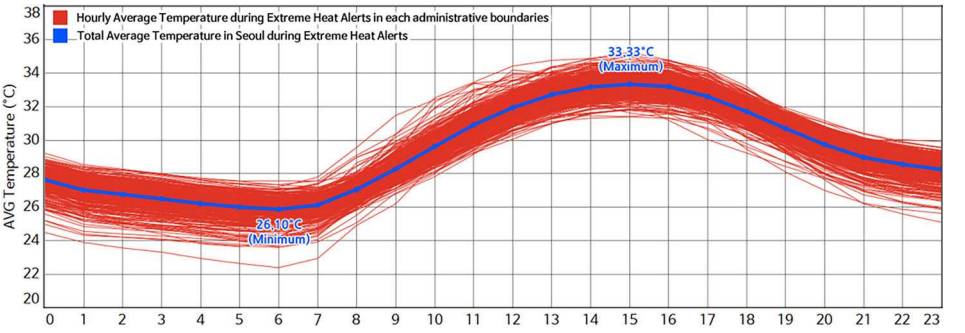

Figure 2. Hourly average temperature during extreme heat alerts in each administration boundaries in Seoul, South Korea.

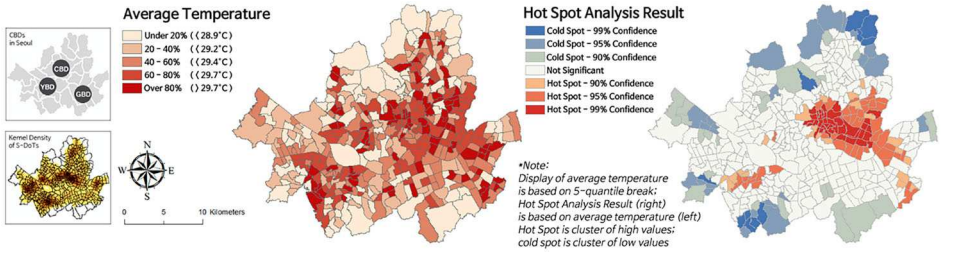

Figure 3. Average temperature and hot spot analysis during extreme heat alerts by administration boundaries in Seoul, South Korea.

depending on time zones and administrative dongs mean that the deviation of extreme heat risk is spatiotemporally different.

The results of the temporal hot spot analysis for temperature during peak and off-peak hours are presented in Figure 4. It is based on the average hourly temperature recorded during advisory alerts. The peak hours are defined as the period from 12 pm to 6 pm, and the off-peak hours encompass all other times. During peak hours, clusters of hot spots were identified in the Eastern part of Seoul. During off-peak hours, the most prominent hot spots were observed in Seoul's East-central and Southwestern regions.

4.2. Validation of S-DoT: temperature comparison between S-DoT and LST

Figure 5 depicts an LST map computed from a satellite image and a temperature map determined for each S-DoT created by spatial interpolation. In data collection, due to the low continuity in the orbital cycle (16 days) of the mid-resolution Landsat 8 and the higher cloud ratio in the summertime during the rainy season (from June to July) in Korea, we found that it is not easy to obtain the recent satellite images that measured the temperature of each region. The LST and the S-DoT temperature map show a similar pattern, with higher values in the northeast and southeast area, while the north-central area, mainly hills and mountains, show lower values. In addition, some areas without S-DoT sensors represent lower temperatures when interpolating, having higher values in the LST map. Significantly, this disparity appears in the part of the western area.

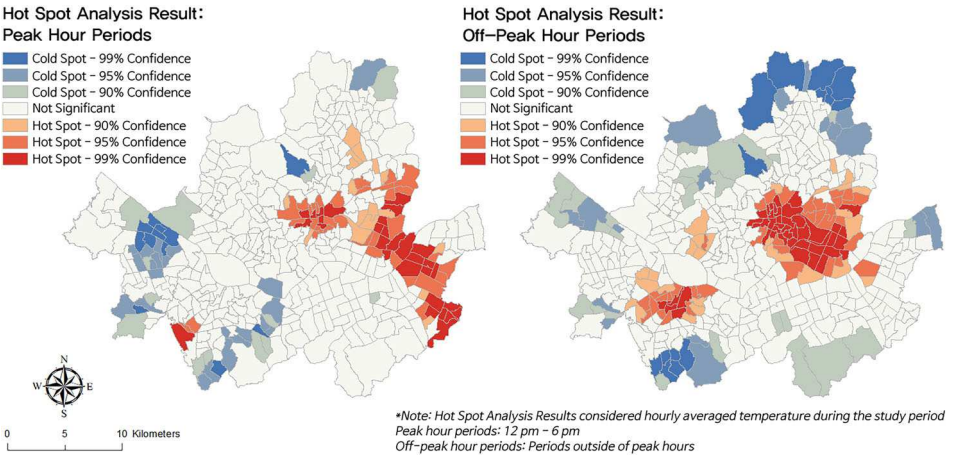

Figure 4. Temporal hot spot analysis during extreme heat alerts by administration boundaries in Seoul, South Korea.

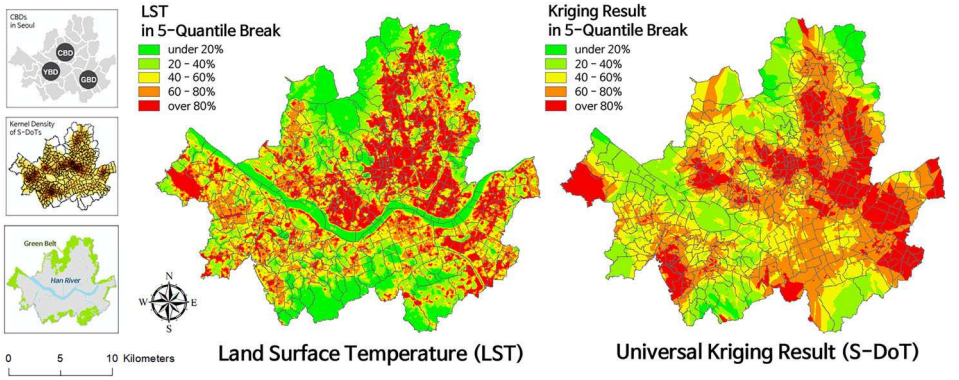

Figure 5. Temperature comparison between land surface temperature (LST) and S-DoT sensors.

Correlation analysis was performed using fishnet points to identify the similarity in the LST and the S-DoT temperature map (Figure 6).[2] The Pearson's correlation coefficient is 0.3369, indicating a moderate positive relationship between the two maps ($p < 0.000$).

4.3. *Heat risk assessment*

The Z-score analysis by the averaged administrative dong used in the heat risk analysis shows differences in heat exposure by age (Figure 7). For each of the youth, working, and elderly groups, there are 43 low-risk and 42 high-risk regions, respectively. The working group is relatively exposed in downtown Seoul (CBD) compared to the youth and the elderly group, showing a lower heat exposure on the outskirts of the city. The exposure of the elderly group to heatwaves is relatively high in the northern part of Seoul. Meanwhile, the heat exposure of the youth group shows a scattered pattern throughout the residential areas in Seoul, with relatively low exposure in the downtown area. The results suggest an apparent geographical disparity in heat exposure by age group.

This study conducted an independent T-Test to examine the statistical difference between the lowest and highest heat-exposed area by age group. We primarily focused

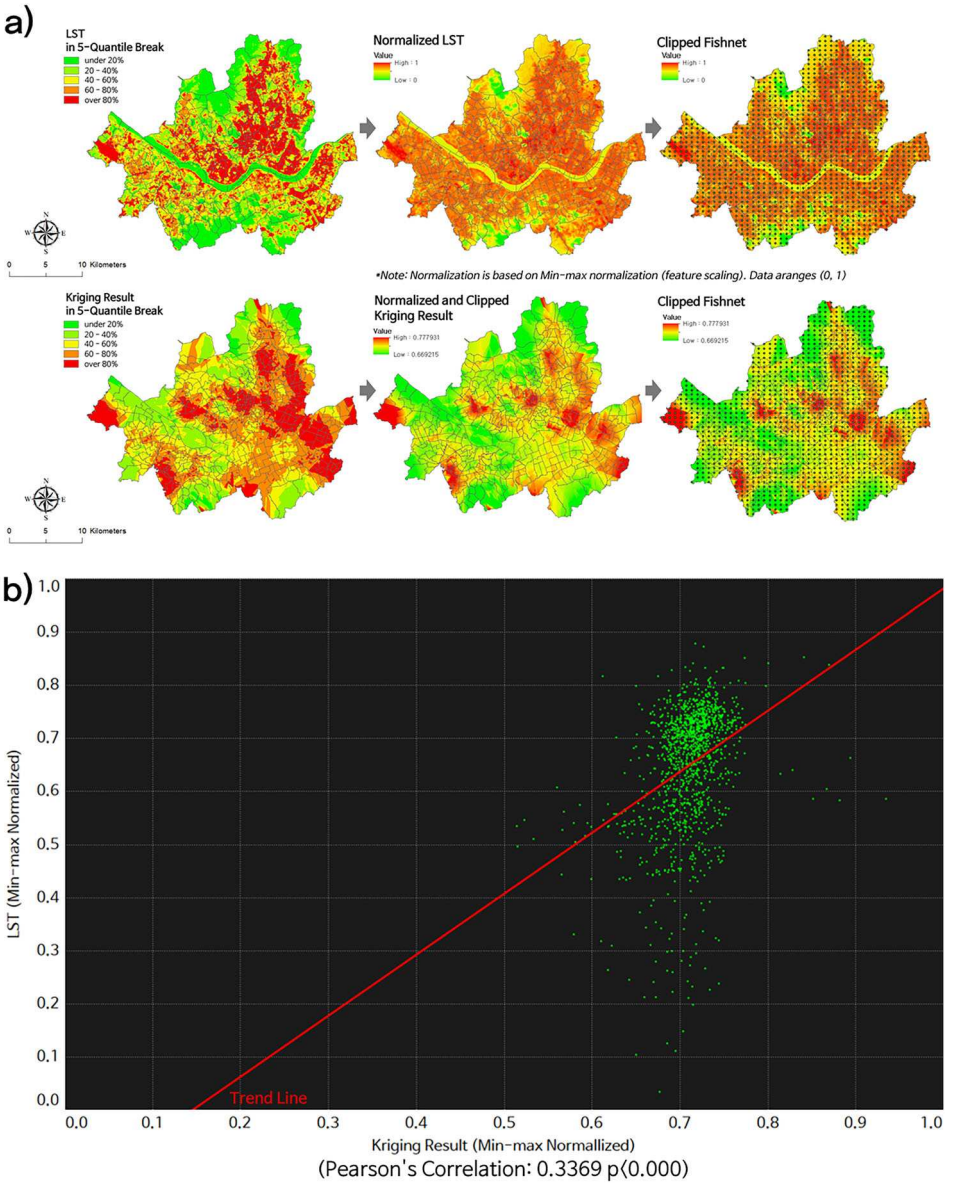

Figure 6. (a) Pre-processing LST and kriging result before correlation analysis, (b) the result of Pearson's correlation.

on variables closely related to the capability to withstand extreme heat. Notably, the urban greenness factor considers the number of parks, park area per person, city park area per person, and walkable park area per person across administrative boundaries in Seoul. In addition, the number of public heat shelters to evade extreme heat per person was considered. The Seoul Metropolitan Government provides a list of officially designated public heat shelters, which are open for public access to help citizens escape extreme heat and stay cool. This data is publicly available.

The T-Test result (Table 2) shows the overall significant difference between the lowest and highest risk areas in age groups relevant to human dynamics data. The

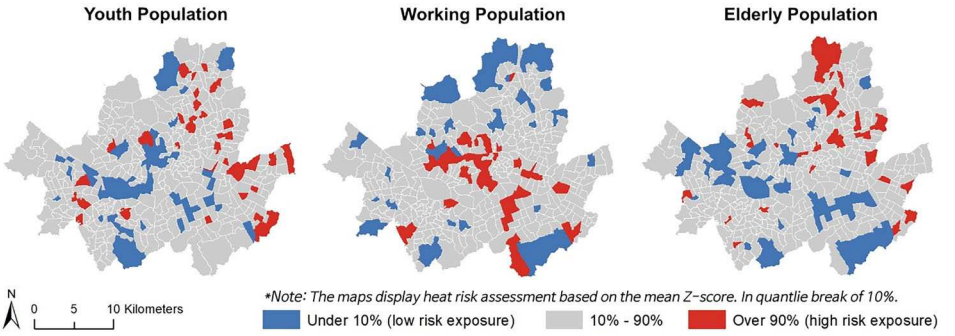

Figure 7. Heat risk assessment by age group.

Table 1. Descriptive statistics.

Variables			Count	Mean	Std	Min	Median	Max
S-DoT (Seoul Metropolitan Government 2021b)	Climate factors	Average temperature (°C)	10,176	29.29	2.65	22.40	28.88	35.23
Human dynamics (Seoul Metropolitan Government 2021a)	During extreme heat advisory alerts	Youth population (%)	10,176	0.10	0.04	0.01	0.10	0.26
		Elderly population (%)	10,176	0.16	0.03	0.06	0.16	0.29
		Working population (%)	10,176	0.74	0.06	0.60	0.73	0.93

highest risk areas demonstrated a larger proportion of respective age groups. For example, regions with the highest risk for the youth group had a significantly higher proportion of youth human dynamics than those regions at the lowest risk. A similar pattern was observed in the working and elderly groups. Regarding vulnerable populations, the number of elderly people living alone, registered people with disabilities, low-income voucher recipients, and people with severe medical conditions is statistically higher in areas where the elderly population are at risk of heat. The number of people with disabilities is also higher in the areas with higher risk to the youth group.

The areas with the highest risk in the working group have a significant number of temporal workers who primarily work in the outdoor construction field than the lowest heat risk areas. These results indicate that vulnerable groups share similar burdens concerning significant heat risks.

Regarding urban greenness, the regions with the highest heat risk comprised fewer number and areas of parks, areas of city parks, and walkable parks per person than the lowest heat risk regions in the youth population group ($p < 0.01$). The results were found in the areas with highest heat risk for the elderly group except the per person park area. Meanwhile, the result suggests that the number of parks is limited in high-risk areas for the working group ($t = -2.149$, $p < 0.05$).

In addition, there is no statistical difference between the highest and lowest heat exposed areas in all age groups regarding the number of public heat shelters to evade

Table 2. T-test result between the highest and lowest vulnerable regions in age groups.

Variable			Youth		Working		Elderly	
			t	*p*	t	*p*	t	*p*
Socio-demographic factor	Vulnerable population	Elderly living alone	0.751	0.454	−3.767	0.000***	8.385	0.000***
		Youth head of the household	−1.035	0.302	−2.227	0.027*	0.332	0.741
		Registered people with disabilities	2.855	0.005**	−5.809	0.000***	6.361	0.000***
		Low-income voucher recipients	1.737	0.084	−3.708	0.000***	7.916	0.000***
		Population with severe pre-medical conditions	−1.703	0.090	−2.856	0.005**	2.678	0.008**
		Temporal workers	−2.223	0.028*	2.974	0.003**	−4.814	0.000***
		Household living alone	2.139	0.034*	−1.783	0.076	−0.210	0.834
Urban greenness factor		Number of parks	−2.841	0.005**	−2.149	0.033*	−3.439	0.001**
		Area of park per person	−2.540	0.012**	−1.484	0.140	−0.488	0.627
		Area of city park per person	−2.871	0.005**	−0.611	0.542	−2.751	0.007**
		Area of walkable park per person	−3.110	0.002**	0.004	0.997	−3.184	0.002**
Infrastructure factor		Number of public heat shelters to evade extreme heat per person	−0.506	0.614	−2.005	0.049*	−0.991	0.324
Human dynamics		The proportion of human dynamics under age 14 during peak hour periods (12 pm to 6 pm)	9.896	0.000***	−12.890	0.000***	−0.193	0.848
		The proportion of human dynamics age 15 to 64 during peak hour periods (12 pm to 6 pm)	−8.634	0.000***	18.447	0.000***	−6.082	0.000***
		The proportion of human dynamics age over 65 during peak hour periods (12 pm to 6 pm)	2.651	0.010*	−9.932	0.000***	13.349	0.000***

Note. $^{*}p < 0.05$, $^{**}p < 0.01$, $^{***}p < 0.001$.

extreme heat. While only the highest risk areas for the working group statistically have fewer public heat shelters, the youth and elderly groups, who are also more exposed to extreme heat, tend to have comparatively less access to these public facilities designed for heat relief.[3]

Our results suggest that heat vulnerability could be enhanced when combined with numerous socioeconomic elements and urban environmental factors, calling for customized policies and mitigation strategies for the risk of overburdened populations.

4.4. *Application of IoT sensors: case study on anomaly detection*

We explored a pilot case study of one of the administrative boundaries, Changsin-Dong, to better understand the various roles IoT sensors may play in regard to extreme heat events. Changsin-Dong is where low-income elderly have been historically densely located (known as "Jjok-Bang" in local terms) over the years. There are three administrative boundaries in Chansin-Dong. It has not been widely introduced in international studies. The residents live in a single room of less than 71 sqft packed together in multi-dwelling units in poorly managed, old facilities. The shared bathroom and dilapidated housing conditions comprise insanitary conditions, aggravating their risk of extreme heat exposure. Figure 8 shows that the residents in Changsin-Dong are exposed to relatively higher LST and temperatures in peak hour periods.

As our study found that extreme heat occasionally occurs in August, and the fact that Changsin-Dong is relatively exposed to higher LST and meteorological temperature, we conducted anomaly detection in this area, using temperatures observed by S-DoTs in August. Our IForest defined anomal instances of extreme heat that exist in Changsin-Dong. Specifically, if we define the outlier of temperature as the mean temperature in peak hours in Seoul, the model reported 32% accuracy. However, if we define the outlier of temperature greater than the standard of initiating extreme heat alert, the model reported 100% accuracy. Figure 9 illustrates the hourly stamp of identified anomalies greater than the threshold value of the standard in Changsin-Dong. The extreme heat anomalies occurred on 25 and 26 August, centered at 3 pm. These periods were authentically the case when the extreme heat advisory alert was initiated and the temperature was primarily extreme (see Appendix 1 and Figure 2).

In addition, three administrative boundaries in Chansin-Dong reported having only one park, respectively, while the average number of parks in Seoul's administrative

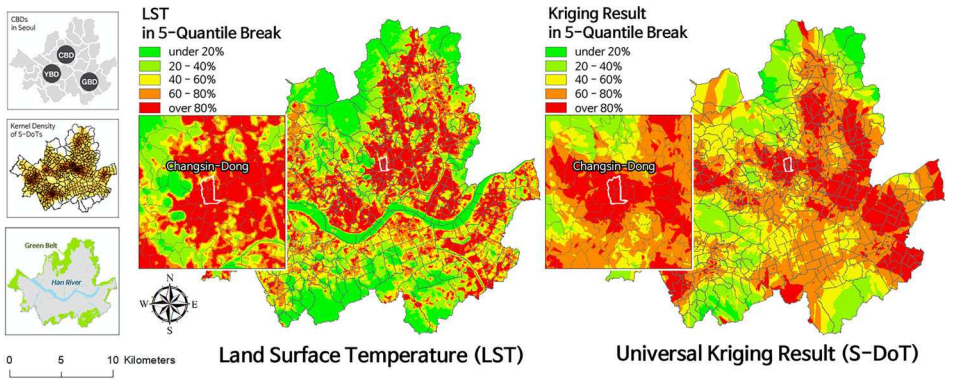

Figure 8. Land surface temperature (LST) and S-DoT temperature comparison in Case area (Changsin-Dong).

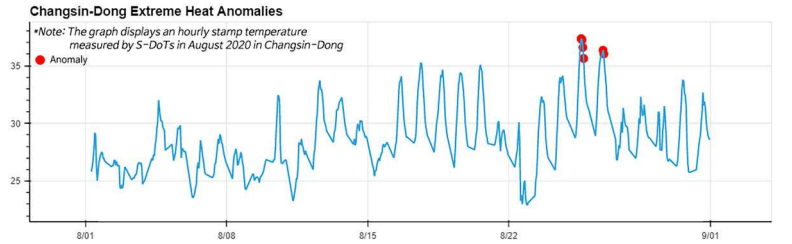

Figure 9. Extreme heat anomaly detention using S-DoTs in Changsin-Dong, Seoul, South Korea.

boundaries is seven. Their mean area of the park (0.77 m^2), city park (0.43 m^2), and walkable park (0.21 m^2) per person were also below the average for all geographic units (see Appendix 2). The average number of public centers in Chansin-Dong (0) was below the city's average (4).

5. Discussion

This study investigates the enhanced use of IoT sensors in assessing the risk of extreme heat events. By combining telecommunication human dynamics data to compute heat exposure by age group, this study analyzed spatiotemporal risks relevant to extreme heat. Also, our study integrated a machine learning toolkit to address whether anomalous instances of extreme heat occur in Seoul.

First, this study revealed the necessity for tailored, localized responses to extreme heat, focusing on interventions that specifically cater to the unique spatiotemporal risk patterns observed among different age groups in urban settings (e.g. green spaces for the elderly or cool roofing materials for young adults working peak daytime hours), to effectively mitigate the impacts of these events. Our results corroborate the previous studies on urban heat intensity, addressing that urban areas exhibit their regional features, despite an outstanding diurnal cycle (a period of one day) (Kim and Baik 2004; Runnalls and Oke 2000). Thus, it is crucial for policymakers to develop strategies that focus on addressing particular risks, suggesting extreme heat mitigation actions in specific regions spatially to reduce influencing factors while focusing on peak hours of vulnerable populations temporally.

Second, IoT sensors offer potential benefits when used in conjunction with existing temperature data. Satellite images are regarded as reliable sources, having been managed and verified over many years. While they allow for the evaluation of historical temperature changes through long-term accumulated data, they do face issues with data continuity. IoT sensors, in contrast, are embedded in living environments to capture changes in urban areas, providing high-resolution data. However, they present challenges in handling outliers or missing data because its formats are close to raw data stored without verification. Furthermore, the limitation exists on analysis that can be employed owing to its short deployment period. In this manner, we suggest researchers understand the pros and cons of each data collection means and choose which data to use depending on the objective of the research, with consideration of potential approaches including data fusion, data interpolation, or model training. The effectiveness of these methods would be dependent on the availability and quality of the IoT sensor data and other data sources. However, we envision that the integration

of IoT sensors would not only bolster our current temperature data but also provide a more comprehensive, dynamic representation of urban thermal patterns. This novel combination of high spatial resolution from LST data and high temporal resolution from IoT sensors, while challenging, holds great promise in refining our understanding of urban heat phenomena and informing targeted mitigation strategies.

In considering the implementation of IoT systems in economically constrained environments, particularly in the Global South, definitive conclusions on feasibility remain elusive due to variations in cost and infrastructure needs. However, initiating pilot projects in areas of critical need could provide a valuable investigation into the environmental benefits of such systems. Concurrently, it allows us to tackle cost-related challenges and explore solutions suitable for these environments. This nuanced approach encourages adaptability, offering the potential to tailor smart solutions to meet unique regional needs and constraints.

Third, our results show that cold spots of heat risk are geographically identified around the outskirts of Seoul. Most of them are designated as development-restricted zones and compose relatively higher greenness than urban centers. The result is in accordance with previous studies arguing that urban greenness (i.e. parks, vegetation, green roofs) reduces damage associated with extreme climate events (Paoletti *et al.* 2011) and contributes to beneficial impacts on mitigating extreme heat events (Van Ryswyk *et al.* 2019). Despite its positive impact on increasing climate adaptive capacity, our risk assessment demonstrated that the highest heat-exposed regions for youth and the elderly groups have fewer parks. Hazard mitigation policies often purposely or unintentionally favor specific communities, disproportionately providing resources and services (Seong, Losey, and Gu 2022). Our results call for actions toward equitable landscape design and ecological solutions regarding urban greenness.

Fourth, our findings suggest that human activity is not evenly distributed in heat-exposed areas only by age group but may contextually coexist with other climate-vulnerable groups. This suggests the need for urgent measures and efforts in such areas. However, it is crucial to note that this data does not provide explicit information on the nature of the stay (indoors or outdoors) of this population in these areas, which is a limitation of our study. Our results corroborate previous studies addressing that social isolation, poverty, and disabilities – possibly due to pre-existing morbidity and reduced mobility conditions – are significant factors that increase elderly vulnerability to extreme heat (Nayak *et al.* 2018). In addition, our results indicate elevated risks among outdoor workers (primarily temporal workers in South Korea) in high-risk areas for working groups. This conclusion is primarily based on demographic data and the common industries in these high-risk regions. However, we acknowledge the occupational diversity within human activity, including a significant proportion that could be involved in the service sector and other industries. Therefore, the conclusions drawn are not intended to oversimplify this diversity. Policymakers should be aware of those socio-demographic overlaps as contextual factors related to higher climate risks. Also, programs and initiatives should focus on socio-ecological solutions for disadvantaged populations in highly heat-exposed areas. More precise risk assessments would benefit from more granular data on the occupations and specific human activities, which is an area for future research.

Finally, our IForest model identified that anomalous instances of extreme heat do occur in vulnerable regions in Seoul. Extreme anomalous cases were reported when extreme heat alerts were initiated, and the temperature was relatively at the highest in time periods. Given this fact, integrating the IoT sensors into environmental assessment

contributes to helping monitor the degree of climate risk across the city concurrently. Now that a significant quantity of sensors have been installed, policymakers and local government agencies should move on to the phases that contemplate integrating the sensors' findings into their initiatives. One option is combining technical findings through recent machine learning toolkits with local knowledge to build collaborative initiatives and work with local grassroots organizations through bottom-up approaches. It may allow local stakeholders to actively participate in the environmental issues based on open data-driven evidence and suggest solutions considering their local context.

6. Conclusion

This study is the first to use exceptionally high-resolution data sources to uncover climate risks caused by extreme heat events and integrate them with human dynamics data, considering risks as chronic pressures on urban populations. Our findings suggest that the unequal distribution of climate exposure risks across age groups must be explicitly addressed for equitable urban resilience planning.

This article contributes to a growing literature on evaluating risks related to extreme heat using innovative data sources and technologies. Given that we used publicly available data (S-DoTs, mobile phone signal-based human dynamics data), our approach is replicable to address other forms of climate vulnerability in other cities deploying IoT sensors and real-time mobile data. Global smart city initiatives involve the utilization of urban climate sensors (Ahn, Lee, and Hong 2022). Microsoft air quality sensors in Chicago and Miami, USA (Microsoft 2021), the Smart Nation Sensor Platform in Singapore, and Google Street View vehicles from Google (Google 2022) are excellent examples of how urban sensors may be used. Given that, our study could provide a reference case of IoT applications for extreme weather events.

There are several limitations to note. First, S-DoT sensors may recall biased results as their operation has not yet been fully validated. The likelihood of hardware failure, overheating, and signal glitches should be further investigated. Second, the study draws from human dynamics data sourced exclusively from one telecommunications company, potentially limiting its representation of the broader mobile phone user base. Third, certain demographic groups, including the elderly, young children, and infants, may not own mobile phones, suggesting that the mobile phone data could fail to accurately mirror the demographic composition of the entire population within the study area. To mitigate these limitations and enhance the accuracy of our analysis, our human dynamics data was adjusted based on the census data, aiming to better reflect the true demographic composition of the study area. Fourth, we used a standardized Z-score to analyze heat risk exposure. However, it does not fully incorporate the spatial mismatch and structural disparity issues. Fifth, the independent T-Test conducted only reveals the statistical difference between the highest and lowest heat risk regions. Additional studies should subsequently seek the correlations and impacts of determinant factors on calculated vulnerability. We also leave deep dive into the analysis and validation of S-DoT sensors as a task for future studies.

Acknowledgements

A part of this manuscript is a revised draft of Seung Jun Choi's Master's degree-professional report at The University of Texas at Austin published in April 2022.

Disclosure statement

No potential conflict of interest was reported by the author(s).

Notes

1. We acknowledge the challenges encountered in finding satellite images that corresponded to the desired period. These challenges include limitations in selecting multiple Landsat images and creating a mosaic image during the same period. When selecting the Landsat 8 image, we had two significant rationales: (1) Images with cloud coverage less than 20% to address the potential errors introduced by clouds; (2) Dates corresponding to the specific day designated as an extreme heat advisory alert by the Korea Meteorological Administration. However, none of the Landsat images obtained during the study period coincided with these designated days. We expanded our search and selected alternative images that aligned with the specified rationales, focusing on the summer period, spanning from May to September, between the years 2017 and 2023. Remarkably, we found that the Landsat 8 image acquired on 23 June 2017 was the only image that fulfilled both rationales and aligned with the requirements of this study. We recognize that limited availability of Landsat images on the exact dates of interest can impact the representativeness and accuracy of the comparison. To address the limitations, we implemented a data normalization approach. By normalizing the LST values from the Landsat image and the S-DOT average air temperature data to a common baseline, we account for the temporal and spatial differences between the datasets.
2. We aggregated the temperature data for each dong and the correlation coefficient between LST and S-DoT aggregated was found to be 0.223, which was lower than the correlation coefficient obtained using fishnet points. This difference in correlation strength can be attributed to the loss of finer spatial variations in temperature when aggregating the data. We found out the benefit of using fishnet points in capturing localized temperature relationships that may be missed with aggregated data.
3. Public heat shelters, often known as cooling centers or cooling facilities, are establishments that receive financial support from governments to cover air conditioning expenses and operational costs. These centers are specifically designed to create a cool environment, particularly for vulnerable populations such as senior citizens, children, and individuals at higher risk, during the summer season.

Funding

This work was supported by National Science Foundation under Grant [NSF-2125858; 2133302; 1952193]; The UT Good System Grand Challenge under Grant [Good Systems]; The USDOT Cooperative Mobility for Competitive Megaregions University Transportation Center at The University of Texas at Austin under Grant [USDOT CM2].

References

Ahn, Haesung, Jeongwoo Lee, and Andy Hong. 2022. “Urban Form and Air Pollution: Clustering Patterns of Urban Form Factors Related to Particulate Matter in Seoul, Korea.” *Sustainable Cities and Society* 81 (June): 103859. doi:10.1016/j.scs.2022.103859.

Aubrecht, Christoph, Klaus Steinnocher, Mario Köstl, Johann Züger, and Wolfgang Loibl. 2013. “Long-Term Spatio-Temporal Social Vulnerability Variation Considering Health-Related Climate Change Parameters Particularly Affecting Elderly.” *Natural Hazards* 68 (3): 1371–1384. doi:10.1007/s11069-012-0324-0.

Avdan, Ugur, and Gordana Jovanovska. 2016. “Algorithm for Automated Mapping of Land Surface Temperature Using LANDSAT 8 Satellite Data.” *Journal of Sensors* 2016(February): E 1480307–E 1480308. doi:10.1155/2016/1480307.

Barbour, Edward, Carlos Cerezo Davila, Siddharth Gupta, Christoph Reinhart, Jasleen Kaur, and Marta C. González. 2019. “Planning for Sustainable Cities by Estimating Building

Occupancy with Mobile Phones." *Nature Communications* 10 (1): 3736. doi:10.1038/s41467-019-11685-w.

Basu, Rupa, and Bart D. Ostro. 2008. "A Multicounty Analysis Identifying the Populations Vulnerable to Mortality Associated with High Ambient Temperature in California." *American Journal of Epidemiology* 168 (6): 632–637. doi:10.1093/aje/kwn170.

Baz-Lomba, Jose Antonio, Francesco Di Ruscio, Arturo Amador, Malcolm Reid, and Kevin V. Thomas. 2019. "Assessing Alternative Population Size Proxies in a Wastewater Catchment Area Using Mobile Device Data." *Environmental Science & Technology* 53 (4): 1994–2001. doi:10.1021/acs.est.8b05389.

Bytomski, Jeffrey R., and Deborah L. Squire. 2003. "Heat Illness in Children." *Current Sports Medicine Reports* 2 (6): 320–324. doi:10.1249/00149619-200312000-00007.

Caballero, William, Ramón Giraldo, and Jorge Mateu. 2013. "A Universal Kriging Approach for Spatial Functional Data." *Stochastic Environmental Research and Risk Assessment* 27 (7): 1553–1563. doi:10.1007/s00477-013-0691-4.

Chakraborty, T. C., Andrew Newman, Yun Qian, Angel Hsu, and Glenn Sheriff. 2022. *Residential Segregation and Urban Heat Stress Disparities in the United States.* Rochester, NY: SSRN Scholarly Paper. doi:10.2139/ssrn.4231649.

Chen, Zifeng, and Anthony Gar-On Yeh. 2022. "Delineating Functional Urban Areas in Chinese Mega City Regions Using Fine-Grained Population Data and Cellphone Location Data: A Case of Pearl River Delta." *Computers, Environment and Urban Systems* 93 (April): 101771. doi:10.1016/j.compenvurbsys.2022.101771.

Cho, Seonga, and Gunhak Lee. 2022. "Spatiotemporal Multi-Objective Optimization for Competitive Mobile Vendors' Location and Routing Using De Facto Population Demands." *Geographical Analysis* 54 (2): 294–308. doi:10.1111/gean.12292.

Christenson, Megan, Sarah Dee Geiger, Jeffrey Phillips, Ben Anderson, Giovanna Losurdo, and Henry A. Anderson. 2017. "Heat Vulnerability Index Mapping for Milwaukee and Wisconsin." *Journal of Public Health Management and Practice: JPHMP* 23 (4): 396–403. doi:10.1097/PHH.0000000000000352.

Depietri, Yaella, Torsten Welle, and Fabrice G. Renaud. 2013. "Social Vulnerability Assessment of the Cologne Urban Area (Germany) to Heat Waves: Links to Ecosystem Services." *International Journal of Disaster Risk Reduction* 6 (December): 98–117. doi:10.1016/j.ijdrr.2013.10.001.

ESRI. 2023. "Hot Spot Analysis (Getis-Ord Gi*) (Spatial Statistics)." Accessed December 2, 2022. https://pro.arcgis.com/en/pro-app/latest/tool-reference/spatial-statistics/hot-spot-analysis.htm

Fauzandi, Fachri Ilman, Yulia Retnowati, Josua Dion Tamba, Emir Mauludi Husni, Rahadian Yusuf, and Bernardo Nugroho Yahya. 2021. "Design and Implementation of Low Cost IoT Sensor System for Urban Heat Island Observation." In *2021 International Conference on Electrical Engineering and Informatics (ICEEI)*, 1–6. New York: IEEE. doi:10.1109/ICEEI52609.2021.9611099.

Google. 2022. "How Street View Works and Where We Will Collect Images Next." *Google Maps Street View*. Accessed 2 December 2022. https://www.google.com/streetview/how-it-works/

Ha, Kyung-Ja, and Kyung-Sook Yun. 2012. "Climate Change Effects on Tropical Night Days in Seoul, Korea." *Theoretical and Applied Climatology* 109 (1-2): 191–203. doi:10.1007/s00704-011-0573-y.

Harris, Charles R., K. Jarrod Millman, Stéfan J. van der Walt, Ralf Gommers, Pauli Virtanen, David Cournapeau, Eric Wieser, *et al.* 2020. "Array Programming with NumPy." *Nature* 585 (7825): 357–362. doi:10.1038/s41586-020-2649-2.

Hasan, M., Md. M. Islam, M. I. I. Zarif, and M. M. A. Hashem. 2019. "Attack and Anomaly Detection in IoT Sensors in IoT Sites Using Machine Learning Approaches." *Internet of Things* 7: 100059. doi:10.1016/j.iot.2019.100059.

Hudson, Gordon, and Hans Wackernagel. 1994. "Mapping Temperature Using Kriging with External Drift: Theory and an Example from Scotland." *International Journal of Climatology* 14 (1): 77–91. doi:10.1002/joc.3370140107.

Husni, Emir, Galang Adira Prayoga, Josua Dion Tamba, Yulia Retnowati, Fachri Imam Fauzandi, Rahadian Yusuf, and Bernardo Nugroho Yahya. 2022. "Microclimate Investigation of Vehicular Traffic on the Urban Heat Island through IoT-Based Device." *Heliyon* 8 (11): E 11739. doi:10.1016/j.heliyon.2022.e11739.

Kang, Chang-Deok. 2020. “Effects of the Human and Built Environment on Neighborhood Vitality: Evidence from Seoul, Korea, Using Mobile Phone Data.” *Journal of Urban Planning and Development* 146 (4): 05020024. doi:10.1061/(ASCE)UP.1943-5444.0000620.

Kim, Do-Woo, Jea-Hak Chung, Jong-Seol Lee, and Ji-Sun Lee. 2014. “Characteristics of Heat Wave Mortality in Korea.” *Atmosphere* 24 (2): 225–234. doi:10.14191/Atmos.2014.24.2.225.

Kim, Do-Woo, Ravinesh C. Deo, Jea-Hak Chung, and Jong-Seol Lee. 2016. “Projection of Heat Wave Mortality Related to Climate Change in Korea.” *Natural Hazards* 80 (1): 623–637. doi:10.1007/s11069-015-1987-0.

Kim, Do-Woo, Ravinesh C. Deo, Jong-Seol Lee, and Jong-Min Yeom. 2017. “Mapping Heatwave Vulnerability in Korea.” *Natural Hazards* 89 (1): 35–55. doi:10.1007/s11069-017-2951-y.

Kim, Jisu, and Min Gyu Kang. 2022. “A Study on the Micro-Scale Heat Wave Vulnerability Assessment Using Urban Data Sensors (S-DoT) in Seoul.” *Journal of Korea Planning Association* 57 (5): 215–234. doi:10.17208/jkpa.2022.10.57.5.215.

Kim, Kijung, and Youngsoo An. 2017. “An Empirical Study on the Definition and Classification Methodology of Urban Heat Island Areas.” *Journal of the Korean Regional Science Association* 33 (2): 47–59. doi:10.22669/krsa.2017.33.2.047.

Kim, Kyung-Hye, and Jang Dong Yeol. 2015. *The 2015 Seoul Welfare Survey: An In-Depth Analysis Report.* Seoul, S. Korea: The Seoul Institute.

Kim, Y.-H., and J.-J. Baik. 2004. “Daily Maximum Urban Heat Island Intensity in Large Cities of Korea.” *Theoretical and Applied Climatology* 79 (3-4): 151–164. doi:10.1007/s00704-004-0070-7.

Korea Institute for Health and Social Affairs. 2020. *Adaptation to the Health Effects of Heat Waves in Sensitive Groups*. Sejong City: Korea Institute for Health and Social Affairs.

Krous, Henry F., Julie M. Nadeau, Richard I. Fukumoto, Brian D. Blackbourne, and Roger W. Byard. 2001. “Environmental Hyperthermic Infant and Early Childhood Death: Circumstances, Pathologic Changes, and Manner of Death.” *The American Journal of Forensic Medicine and Pathology* 22 (4): 374–382. LWWdoi:10.1097/00000433-200112000-00008.

Ku, Chayong. 2014. “Development of Land Surface Temperature Map Generation Method with Landsat 8 TIRS Imagery and Automatic Weather System Data.” *Journal of Korean Cartographic Association* 14 (1): 17–27.

Kwon, You Jin., Dong Kun Lee, and You Ha Kwon. 2020. “Is Sensible Heat Flux Useful for the Assessment of Thermal Vulnerability in Seoul (Korea)?” *International Journal of Environmental Research and Public Health* 17 (3): 963. MDPIdoi:10.3390/ijerph17030963.

Lee, Hye Kyung, Junfeng Jiao, and Seung Jun Choi. 2021. “Identifying Spatiotemporal Transit Deserts in Seoul, South Korea.” *Journal of Transport Geography* 95 (July): 103145. doi:10.1016/j.jtrangeo.2021.103145.

Lee, Hyekyung, Seungjun Choi, and Junfeng Jiao. 2021. “Examining the COVID-19 Effects on Travel Behavior Using Smart IoT Sensors: A Case Study of Smart City Planning in Gangnam, Seoul.” *International Journal of Sustainable Building Technology and Urban Development* 12 (4): 347–362. doi:10.22712/SUSB.20210029.

Lee, Won Kyung, Hye Ah Lee, Youn Hee Lim, and Hyesook Park. 2016. “Added Effect of Heat Wave on Mortality in Seoul, Korea.” *International Journal of Biometeorology* 60 (5): 719–726. doi:10.1007/s00484-015-1067-x.

Liu, Fei Tony, Kai Ming Ting, and Zhi-Hua Zhou. 2008. “Isolation Forest.” In *2008 Eighth IEEE International Conference on Data Mining*, 413–422. New York: IEEE. doi:10.1109/ICDM.2008.17.

Microsoft. 2021. “Project Eclipse.” Microsoft Research. Accessed 1 October 2021. https://www.microsoft.com/en-us/research/project/project-eclipse/

Muller, Catherine L., Lee Chapman, C. S. B. Grimmond, Duick T. Young, and Xiaoming Cai. 2013. “Sensors and the City: A Review of Urban Meteorological Networks.” *International Journal of Climatology* 33 (7): 1585–1600. doi:10.1002/joc.3678.

Nayak, Seema G., Srishti Shrestha, P. L. Kinney, Zev Ross, S. C. Sheridan, C. I. Pantea, W. H. Hsu, Nicola Muscatiello, and Syni-An Hwang. 2018. “Development of a Heat Vulnerability Index for New York State.” *Public Health* 161: 127–137. doi:10.1016/j.puhe.2017.09.006.

Nica, Elvira. 2021. “Urban Big Data Analytics and Sustainable Governance Networks in Integrated Smart City Planning and Management.” *Geopolitics, History, and International Relations* 13 (2): 93–106.

Paoletti, Elena, Tommaso Bardelli, Gianluca Giovannini, and Leonella Pecchioli. 2011. "Air Quality Impact of an Urban Park over Time." *Procedia Environmental Sciences* 4 (0): 10–16. doi:10.1016/j.proenv.2011.03.002.

Park, Moon-Soo, and Kitae Baek. 2023. "Quality Management System for an IoT Meteorological Sensor Network: Application to Smart Seoul Data of Things (S-DoT)." *Sensors* 23 (5): 2384. doi:10.3390/s23052384.

Park, Keon Chul, and Yoosin Kim. 2020. *Analysis Study on Characteristics and Utilization Directions of Data Collected by the Smart Seoul Data of Things (S-DoT)*. Seoul, S. Korea: Seoul Digital Foundation.

Patel, Keyur K., Sunil M. Patel, and P. G. Scholar. 2016. "Internet of Things-IOT: Definition, Characteristics, Architecture, Enabling Technologies, Application & Future Challenges." *International Journal of Engineering Science and Computing* 6: 6122–6131.

Pedregosa, Fabian, Gaël Varoquaux, Alexandre Gramfort, Vincent Michel, Bertrand Thirion, Olivier Grisel, Mathieu Blondel, *et al.* 2011. "Scikit-Learn: Machine Learning in Python." *The Journal of Machine Learning Research* 12: 2825–2830.

Perkins-Kirkpatrick, S. E., and P. B. Gibson. 2017. "Changes in Regional Heatwave Characteristics as a Function of Increasing Global Temperature." *Scientific Reports* 7 (1): 12256. doi:10.1038/s41598-017-12520-2.

Rathore, M. Mazhar, Awais Ahmad, and Anand Paul. 2016. "IoT-Based Smart City Development Using Big Data Analytical Approach." In *2016 IEEE International Conference on Automatica (ICA-ACCA)*, 1–8. New York: IEEE. doi:10.1109/ICA-ACCA.2016.7778510.

Reback, Jeff., Jbrockmendel, Wes McKinney, Joris Van Den Bossche, Matthew Roeschke, Tom Augspurger, Simon Hawkins, *et al.* 2022. "Pandas-Dev/Pandas: Pandas 1.4.3." Zenodo. https://zenodo.org/records/10537285

Roznik, Mitchell, C. Brock Porth, Lysa Porth, Milton Boyd, and Katerina Roznik. 2019. "Improving Agricultural Microinsurance by Applying Universal Kriging and Generalised Additive Models for Interpolation of Mean Daily Temperature." *The Geneva Papers on Risk and Insurance - Issues and Practice* 44 (3): 446–480. doi:10.1057/s41288-019-00127-9.

Runnalls, K. E., and T. R. Oke. 2000. "Dynamics and Controls of the Near-Surface Heat Island of Vancouver, British Columbia." *Physical Geography* 21 (4): 283–304. doi:10.1080/02723646.2000.10642711.

Sehrawat, Deepti, and N. S. Gill. 2019. "Smart Sensors: Analysis of Different Types of IoT Sensors." In *2019 3rd International Conference on Trends in Electronics and Informatics (ICOEI)*, 523–528. New York: IEEE. doi:10.1109/ICOEI.2019.8862778.

Seong, Kijin, Junfeng Jiao, and Akhil Mandalapu. 2023. "Effects of Urban Environmental Factors on Heat-Related Emergency Medical Services (EMS) Response Time." *Applied Geography* 155 (June): 102956. doi:10.1016/j.apgeog.2023.102956.

Seong, Kijin, Clare Losey, and Donghwan Gu. 2022. "Naturally Resilient to Natural Hazards? Urban–Rural Disparities in Hazard Mitigation Grant Program Assistance." *Housing Policy Debate* 32 (1): 190–210. doi:10.1080/10511482.2021.1938172.

Seoul Metropolitan Government. 2021a. "Seoul Human Dynamics." Accessed December 9, 2022. https://data.seoul.go.kr

Seoul Metropolitan Government. 2021b. "Smart Seoul S-DoT Environmental Information" Accessed December 9, 2022. https://data.seoul.go.kr/dataList/OA-15969/S/1/datasetView.do

Seoul Metropolitan Government. 2022. "Statistics of Seoul Metropolitan City National Basic Livelihood Security Recipients by District." Accessed January 10, 2024. https://data.seoul.go.kr

Sima, Lenka, Yvonne Thomas, and Daniel Lowrie. 2017. "Occupational Disruption and Natural Disaster: Finding a 'New Normal' in a Changed Context." *Journal of Occupational Science* 24 (2): 128–139. doi:10.1080/14427591.2017.1306790.

Smith, Tiffany T., Benjamin F. Zaitchik, and Julia M. Gohlke. 2013. "Heat Waves in the United States: Definitions, Patterns and Trends." *Climatic Change* 118 (3-4): 811–825. doi:10.1007/s10584-012-0659-2.

Smoliak, Brian V., Peter K. Snyder, Tracy E. Twine, Phillip M. Mykleby, and William F. Hertel. 2015. "Dense Network Observations of the Twin Cities Canopy-Layer Urban Heat Island." *Journal of Applied Meteorology and Climatology* 54 (9): 1899–1917. doi:10.1175/JAMC-D-14-0239.1.

Sobrino, José Antonio, and N. Raissouni. 2000. "Toward Remote Sensing Methods for Land Cover Dynamic Monitoring: Application to Morocco." *International Journal of Remote Sensing* 21 (2): 353–366. doi:10.1080/014311600210876.

Song, Chaoming, Zehui Qu, Nicholas Blumm, and Albert-László Barabási. 2010. "Limits of Predictability in Human Mobility." *Science* 327 (5968): 1018–1021. doi:10.1126/science.1177170.

Sun, Xiaoming, Qiao Sun, Minjuan Yang, Xianfeng Zhou, Xiaopan Li, Aiqing Yu, Fuhai Geng, and Yuming Guo. 2014. "Effects of Temperature and Heat Waves on Emergency Department Visits and Emergency Ambulance Dispatches in Pudong New Area, China: A Time Series Analysis." *Environmental Health: A Global Access Science Source* 13 (1):76. doi:10.1186/1476-069X-13-76.

US. Geological Survey. 2018. *Landsat 8 Data Users Handbook*. Washington, DC: US Department of the Interior.

Van Ryswyk, Keith, Natasha Prince, Mona Ahmed, Erika Brisson, J. David Miller, and Paul J. Villeneuve. 2019. "Does Urban Vegetation Reduce Temperature and Air Pollution Concentrations? Findings from an Environmental Monitoring Study of the Central Experimental Farm in Ottawa, Canada." *Atmospheric Environment* 218: 116886. doi:10.1016/j.atmosenv.2019.116886.

Voogt, James. 2007. "How Researchers Measure Urban Heat Islands." In *United States Environmental Protection Agency (EPA), State and Local Climate and Energy Program, Heat Island Effect, Urban Heat Island Webcasts and Conference Calls*. Washington, DC: US Environmental Protection Agency.

Watson, K. E., K. M. Gardiner, and J. A. Singleton. 2020. "The Impact of Extreme Heat Events on Hospital Admissions to the Royal Hobart Hospital." *Journal of Public Health* 42: 333–339. doi:10.1093/pubmed/fdz033.

Wilson, Bev, and Arnab Chakraborty. 2019. "Mapping Vulnerability to Extreme Heat Events: Lessons from Metropolitan Chicago." *Journal of Environmental Planning and Management* 62 (6): 1065–1088. doi:10.1080/09640568.2018.1462475.

Yu, Manzhu, Tracy Shen, and Guido Cervone. 2022. "Chapter 13 - A Comparative Study of Deep Learning-Based Time-Series Forecasting Techniques for Fine-Scale Urban Extreme Heat Prediction Using Internet of Things Observations." In *Nanotechnology-Based Smart Remote Sensing Networks for Disaster Prevention*, edited by Adil Denizli, Marcelo S. Alencar, Tuan Anh Nguyen, and David E. Motaung, 253–271. Micro and Nano Technologies. Amsterdam: Elsevier. doi:10.1016/B978-0-323-91166-5.00014-8.

Zheng, Haiyan, Jinhang Yu, Joongbin Lim, and Kyoo-Seock Lee. 2020. "Spatial and Temporal Characteristics of Tropical Nights in Seoul." *Environmental Monitoring and Assessment* 192 (11): 669. doi:10.1007/s10661-020-08608-4.

Zheng, Minxuan, Jiahua Zhang, Lamei Shi, Da Zhang, Til Prasad Pangali Sharma, and Foyez Ahmed Prodhan. 2020. "Mapping Heat-Related Risks in Northern Jiangxi Province of China Based on Two Spatial Assessment Frameworks Approaches." *International Journal of Environmental Research and Public Health* 17 (18): 6584. doi:10.3390/ijerph17186584.

Appendix 1. Effect date of extreme heat and air pollution advisory alert

Alert	Date in effect
Extreme heat advisory alerts: 17 days (Korea Meteorological Administration)	09 June 2020, 10 June 2020, 21 June 2020, 22 June 2020, 23 June 2020, 12 August 2020, 13 August 2020, 15 August 2020, 16 August 2020, 17 August 2020, 18 August 2020, 19 August 2020, 20 August 2020, 23 August 2020, 24 August 2020, 25 August 2020, 26 August 2020

Appendix 2. Variables and descriptive statistics for T-test.

Variable			Count	Mean	Std	Min	Median	Max
Socio-demographic factor	Vulnerable population (2012–2020)	Elderly living alone (2020)	424	863	401	1	798	2,448
		Youth head of the household (2012)	424	0	1	0	0	4
		Registered people with disabilities (2020)	424	928	496	3	828	3,827
		Low-income voucher recipients (2020)	424	847	667	5	698	5,485
		Population with severe pre-medical conditions (2020)	424	23,424	23,125	1,380	16,730	196,519
		Temporal workers (2019)	424	1,979	5,759	22	977	108,747
		Household living alone (2020)	424	530	295	2	529	999
Urban greenness factor (2020)		Number of parks	424	7	7	1	5	54
		Area of park per person (m^2)	424	1.09	2.08	0.08	0.59	26.75
		Area of city park per person (m^2)	424	0.71	1.16	0.02	0.40	14.73
		Area of walkable park per person (m^2)	424	0.35	0.50	0.04	0.22	7.09
Heat infrastructure factor (2020)		Number of public heat shelters to evade extreme heat	424	4	23	0	6	50